Micro and Nano Scale Sensors for Room Temperature Detection of Methane

by

Mehrnaz Rahimi

A thesis submitted in partial fulfillment of the requirements for the degree of

Master of Science

in

Chemical Engineering

Department of Chemical and Materials Engineering
University of Alberta

Abstract

Detection of methane at room temperature is a challenge due to its inert properties, such as being non polar and showing little tendency to lose or gain electrons at room temperature. Here, we have shown two methods for detection of methane at room temperature via employing micro and nano scale sensing platforms. Nanomechanical IR spectroscopy for methane detection without using any chemoselective interface via measuring the photothermal effect of adsorbed methane on a thermally sensitive cantilever have been used to obtain molecular signature of femto gram quantities of adsorbed methane on the cantilever surface and absorbed mass of methane and residence time have been calculated using the kinetic theory of gases. In the second method a microfabricated interdigitated electrode coated with palladium-single walled carbon nanotubes composites (Pd-SWCNTs) have been used as room temperature methane sensor. Also, fabrications of Pd nanoparticles and incorporation into SWCNTs have been demonstrated.

Acknowledgment

Undoubtedly, many people helped me throughout my graduate studies as a master student and here, I would like to take the opportunity to express my humble gratitude toward them.

First and foremost, I would like to thank my supervisors, Prof. Thomas Thundat and Prof. Sushanta Mitra for giving me the opportunity to work on this project and for all their guidance without which, this work could not have been completed.

I would also like to thank Dr. Mohammad Zarifi for fabrication of IDEs used in this study and also Dr. Dongkyu Lee and Dr. Charles Van Neste for their advice and useful discussions. Next, I'd like to extend my gratitude and appreciation to Ms. Parmiss Mojir Shaibani, Mr. Amirreza Sohrabi, Mr. Eric Hawk for their help and support during this period.

I want to acknowledge Canada Excellence Research Chairs (CERC) program and Carbon Management Canada (CMC) as well for providing financial support during the length of my master's program.

Last, but not least, I would like to thank my wonderful family and friends who have supported me unconditionally through the highs and lows of my graduate studies.

Table of contents

List of Tables

List of Figures

Chapter 1: Introduction and Literature Review

1. Gas sensing

Gas sensing technology is receiving more attention and has become more significant during the past decades due to its broad applications in industrial production , automotive industry, environmental studies, medical applications and indoor air quality supervision [1].

Research in gas sensing can be classified in three different groups [1]:

1. Different kind of sensors
2. Sensing principles
3. Fabrication techniques

Here, different gas sensing methods have been investigated followed by their application in industry and specifically focusing on methane detection at room temperature.

1.1. Gas Sensing Methods

Gas sensing methods can be classified into two main categories: (1) methods based on electrical properties shift; (2) non-electrical based methods [1].

1.1.1. Methods Based on Electrical Properties Shift

1.1.1.1. Metal Oxide Semiconductors

Metal oxides are the most common sensing materials as they have low cost, long life time and can be used for long range of target gases [2]. Precise control of structure and morphology of these materials has made them a fundamental element in smart devices. These materials have two characteristics: (1) cations with mixed valence state; (2) anions with deficiencies. Manipulation of either one or both of these characteristics can tune chemical, electrical, optical and magnetic properties [3].

Metal oxides are divided into two groups of non-transition and transition. The latter has more oxidation states compared to the former which only have one oxidation state, thus can form more oxidation states on the surface and therefore could be used toward gas sensing applications[1], [4].

Semiconductor metal oxide gas sensors can be classified into five groups[3]:

1. Resistive type metal oxide gas sensors
2. Schottky type gas sensors

3. Metal oxide homojunction gas sensors
4. Metal oxide hetrojunction gas sensors
5. Mixed metal oxide gas sensors

The sensing mechanism of metal oxide semiconductors is the redox reaction between the oxide surface and the target gases. The electronic variation of oxide surface, due to distribution of O^- on the surface of material, will result in electrical resistance variation of the sensor. Sensing layer structure and characteristics affect the redox reactions and thus sensitivity of the metal oxide as a gas sensor[1], [4], [5].

Metal oxide semiconductors have advantages such as low cost, short response time, long life time, etc. , however, they have relatively low sensitivity and selectivity. Sensitivity of a metal oxide gas sensor can be improved by methods such as heating, pre-concentrating, using composite materials, etc. On the other hand, selectivity can be enhanced by doping the surface with catalyst material, using sensor arrays, catalytic filtering or compositional control of sensing materials. Another disadvantage of these sensors is their high energy consumption due to their high working temperature that can restrict their development [1], [6].

1.1.1.2. Polymers

Polymers are usually used to detect volatile organic compounds (VOCs) or solvent vapors in the gas phase. However, some research has shown that these materials can be used toward sensing some inorganic gases such as carbon dioxide or H_2O[1], [7]. The sensing mechanism is based on absorption of gas on the polymer layer. Physical properties of the polymer – dielectric constant and mass-change due to gas absorption. Polymers use for gas sensing divided into two class of conducting polymers and non-conducting polymers based upon the physical property change that they undergo.

1.1.1.2.1. Conducting polymers

Electrical properties of these polymers change as they are exposed to different gases and thus they can be used as a gas sensing layer. However, the conductivity of the pure polymer is low and it needs to be increased by either redox reactions or protonation. The doping process makes the polymer either semiconductor or conductor. Most of the polymers are doped by means of redox reactions.

Some of the conducting polymers used toward gas sensing are polyaniline (PAni)[8]–[12], polypyrrole (PPy), polythiophene (PTh) [13].

1.1.1.2.2. Non-conducting polymers

Non-conducting polymers are commonly used as coatings on different devices. The device and the coating are considered as a transducer unit. Non conducting polymers when applied as a molecular sieve on the metal oxide semiconductors can enhance the selectivity of the gas sensing layer since they integrate the sensitivity of polymer layer with the metal oxide layer [1].

Polymers used as gas sensing material offer high sensitivity, short response time, low energy consumption due to their ability to work at room temperature. On the other hand, they have the problem of instability, poor selectivity and irreversibility.

1.1.1.3. Carbon Nanomaterials

Carbon nanomaterials have been attracting a lot of interest and research during the past few years because of their unique electrical,

mechanical and optical properties[14]–[20]. These materials have the potential of being used as gas sensing layers. Their large surface to volume ratio makes these materials highly sensitive. Besides, their adsorption capacity is higher compared to conventional sensing materials and they offer a quick response time. Thus, their electrical properties such as capacitance and resistance can change significantly even when working at room temperature [15],[17],[1]. Most commonly carbon nanomaterials used for developing gas sensors are:

1. Carbon black
2. Carbon nanofibers
3. Carbon nanotubes
4. Garphene

1.1.1.3.1. Carbon black gas sensors

This kind of sensor is made from incorporation of carbon black particles into insulating organic polymers. The electrical conductivity of the polymer film enhances due to dispersion of carbon black. Depending on the amount of carbon black loaded into the polymer, the composites can be either insulator or conductor. The resistivity of

the composite decreases as the amount of carbon black increases, thus composites with low carbon black content are insulators. As the polymer matrix ages the carbon black particles re-aggregate thus making response and baseline drift [17].

1.1.1.3.2. Carbon nanofibers

Carbon nanofibers have high aspect ratio which makes them superior compared to carbon black nanoparticles. These fibers, unlike carbon black nanoparticles, won't move through the polymer matrix during gas adsorption and desorption thus have more stability which results in maintaining their electrical percolation pathways [17].

1.1.1.3.3. Carbon nanotubes

Carbon nanotubes (CNTs) are highly sensitive to environmental change. This feature has made these materials ideal candidates to be used for sensing. Electrical properties of CNTs change with relatively small quantities of gases such as ammonia, carbon dioxide, alcohol and nitrogen oxide (NO_x) at room temperature [17]. Studies have shown that functionalized carbon nanotubes show better chemical bonding between a target chemical species and the nanotube. Also, functionalization enhances the selectivity [21]. Haung et.al [22] have

showed Pd nanoparticle-loaded CNTs have affinity toward hydrogen peroxide and NADH. The interaction between metal nanoparticles and CNTs improves gas detection via change in the electrical conductivity of the nanomaterial. However, decorating CNTs with similar sized metal nanoparticles which are well anchored to CNT sidewalls might be a challenge. One of the techniques to overcome this challenge is using cold reactive plasma treatment. Plasma treatments offer control over the metal nanoparticle size, shape, coordination and diffusion. CNTs can also be functionalized through sputtering [21]. Penza et al. [23] were first to introduce this method for decoration of CNTS with metal nanoparticles.

Other methods which can be employed to enhance selectivity and sensitivity of CNTs are doping and modification of CNTs sidewalls with organic molecules such as DNA. Doping can be done by introducing B and/or N which enhances the conductivity. Nitrogen doped carbon nanotube sensors show response and recovery time of orders of a few seconds toward ammonia [23]. Gelperin et al. [24] found out using DNA coated CNTs can respond to explosives or nerve agent simulants (DNA as the chemical recognition site and single walled CNT as electronic read-out component).

CNTs have the advantages such as being ultra-sensitive, great adsorptive capacity, large aspect ratio, quick response time and low weight. However, they are difficult to fabricate, have high fabrication cost [1].

1.1.1.3.4. Graphene

Novoseloy et al. [25] first demonstrated using grapheme as gas sensor in 2007. Graphene is a low-noise material electronically which makes it an ideal candidate for chemical sensing. When a gas molecule adsorbs or desorbs from graphene's surface, the local carrier concentration changes one by one electron in graphene resulting in step-like changes in resistance [25].

1.1.1.4. Moisture Absorbing Material

Dielectric constant of moisture absorbing materials could be changed when exposed to humidity and water. When embedded with RFID tags, these materials can be used to detect humidity levels. Low cost, low weight and high selectivity to water vapor are some of the

advantages of moisture absorbing materials, whereas vulnerability to friction and being irreversible at high humidity in some cases are some of their drawbacks [1].

1.1.2. Non-Electrical Based Methods

1.1.2.1. Optical Methods

Optical methods also known as spectroscopic methods, since they are mainly based on spectroscopy for gas sensing, offer higher sensitivity, selectivity and stability compared to non-optical methods. These methods can be employed in in on-line real time detections due to their short response time. Spectroscopic analysis is mainly based on absorption and emission spectrometry.

Beer-Lambert law -concentration-dependent absorption of the photons at specific wavelength- forms the principle of absorption spectroscopy [1].

Optical methods can also be classified either as basic absorption spectrometry or improved absorption spectrometry.

Infrared (IR) - source gas sensors are the most widely used gas sensors based on basic absorption spectrometry. Each gas has its own IR absorption finger print which means when exposed to IR radiation; it only absorbs IR at a certain wavelength.

There are three main parts for each IR-source gas sensor:

1. IR source
2. Gas chamber
3. IR detector

Of all the three parts mentioned above, selecting the wavelength range of IR source greatly affects the final detection results. Mid-IR spectral region supports stronger absorption compared to near infrared, but the traditional mid-IR lasers lack continuous wavelength tenability, low output power as well as cooling requirement of lead salt diode lasers, etc. On the other hand, new lasers like Quantum-Cascade Lasers (QCLs) overcome the mentioned disadvantages of traditional mid-IR lasers [1]. QCLs are of interest due to their excellent properties in regard to narrow line width, average power and room temperature operation [26].

Some of the improved absorption spectrometry methods are:

- Tunable Diode Laser Absorption Spectroscopy (TDLAS)
- Raman Light Detection and Ranging (LIDAL)
- Differential Optical Absorption Spectroscopy (DOAS)
- Differential Absorption LIDAR (DIAL)
- Intra-Cavity Absorption Spectrometry (ICAS)

One of the techniques based on emission spectrometry – excited atoms emit photons and go back to the ground state- is Laser Induced Breakdown Spectroscopy (LIBS). Fourier Transform Infrared Spectroscopy (FTIR), Photoacoustic Spectroscopy and Correlation Spectroscopy are also recognizes as spectroscopic analysis.

Optical methods offer high sensitivity, selectivity and stability along with long life time. They are also insensitive to environmental changes, however they have high cost and are difficult to miniaturize [1].

1.1.2.2. Calorimetric Methods

The major class of gas sensors which is considered as calorimetric is pellistor. The word pellistor is combination of pellet and resistor. Pellistors are solid-state devices which have a detecting element that contains a small pellet of catalyst- loaded ceramic. These devices lave

limit of detection (LOD) of low parts per thousand (ppth) thus they are not suitable for laboratory tests. However, they are suitable in industrial applications such as detecting combustible gases. Pellistors can be classified into two groups according to their operating mode: (1) catalytic (2) thermal conductivity [27].

Most of the pellistors made are catalytic type. The target gas is burned in the catalytic mode, thus the resistance in the detecting element changes by the heat generated by burning the gas. The heat produced from burning is proportional to the gas concentration. Catalytic sensors offer high levels of accuracy, short response time and can be incorporated into detection systems. However, the catalyst poisoning due to presence of some impurities in the gas sample, can cause reduced or even irreversible loss of catalyst activities. In the thermal conductivity mode, gases are identified based on the thermal conductivity. Although thermal conductivity sensors have advantages such as reliability, good stability and a large detection range, but their accuracy and sensitivity needs to be improved [1].

1.1.2.3. Gas chromatography

Gas chromatography (GC) is a technique that separates the components of a solution and measures their relative quantities. The use of gas chromatography is limited by the decomposition temperature of the components present in the mixture, thus this method is suitable for chemicals that do not decompose at high temperatures as most of columns cannot operate at temperatures higher than 250-350 ° C [28].

There are several detectors that can be used in GC, however they give different selectivity. Some detectors that are used in GC are:

1. Non-selective detectors
2. Selective detector
3. Specific detector
4. Concentration dependent detector
5. Mass flow dependent detector

Table 1 summarize common GC detectors [29].

GC devices have excellent separation performance, high selectivity and sensitivity but it is difficult to miniaturize besides their high cost. They are usually used in lab. analysis [1].

Table 1.1: summary of common GC detectors [1]

Detector	Type	Support gases	Selectivity	Detectability	Dynamic range
Flame ionization (FID)	Mass flow	Hydrogen and air	Most organic cpds.	100 pg	10^7
Thermal conductivity (TCD)	Concentration	Reference	Universal	1 ng	10^7
Electron capture (ECD)	Concentration	Make-up	Halides, nitrates, nitriles, peroxides, anhydrides, organometallics	50 fg	10^5
Nitrogen-phosphorus	Mass flow	Hydrogen and air	Nitrogen, phosphorus	10 pg	10^6
Flame photometric (FPD)	Mass flow	Hydrogen and air possibly oxygen	Sulphur, phosphorus, tin, boron, arsenic, germanium, selenium, chromium	100 pg	10^3
Photo-ionization (PID)	Concentration	Make-up	Aliphatics, aromatics, ketones, esters, aldehydes, amines, heterocyclics, organosulphurs, some organometallics	2 pg	10^7
Hall electrolytic	Mass flow	Hydrogen, oxygen	Halide, nitrogen,		

conductivity			nitrosamine, sulphur		

1.1.2.4. Acoustic Methods

Acoustic methods have advantages like long lifetime and ability to avoid secondary pollutions. However, they have low sensitivity and are sensitive to environmental changes. This type of sensors can be easily applied into Wireless Sensor Networks (WSN) [1].

Measurements based on ultrasonic methods are classified into three categories of

1. Speed of sound
2. Attenuation
3. Acoustic impedance

From which, the sound velocity is the most popular one. The sound velocity detection method mainly relies on Time-of-Flight (TOF). TOF uses the time of ultrasound travelling from one place to the other, i.e. sound distance, in order to calculate the propagation velocity of ultrasound waves. The measured velocity can determine properties such as:

- Gas concentration based on mathematical reasoning [30]
- Identifying special kind of gases [31]
- Calculating composition or the molar weight of different gases in mixture based on thermodynamics equations [32]

Attenuation which is referred to as the loss of thermal or scattered energy of acoustic wave travelling through a medium is a relatively less robust method. Attenuation combined with sound of speed method, can be used to determine gas properties.

Gas density can be determined using acoustic impedance. Acoustic impedance z, is given by equation (1.1).

$$z = \rho C \quad (1.1)$$

Where ρ is the gas density and C is the sound speed.

Measuring gas impedance is extremely hard thus this method is not very popular from commercial point of view [1].

Table 2 gives a summary of advantages, disadvantages and applications for all the gas sensing methods mentioned in section 2.

Table 1.2: Summary of advantage, disadvantage and application of each gas sensing method [1]

Material	Advantage	Disadvantage	Target Gases and Application Fields
Metal oxide semi-conductor	Low cost; Short response time; Wide range of target gases; Long lifetime	Relatively low sensitivity and selectivity; Sensitive to environmental factors; High energy consumption	Industrial applications and civil use
Polymer	High sensitivity; Short response time; Low cost of fabrication; Simple and portable structure; Low energy consumption	Long-time instability; Irreversibility; Poor selectivity	Indoor air monitoring; Storage place of synthetic products as paints, wax or fuels;
Carbon Nanotubes	Ultra-sensitive; Great adsorptive capacity; Large surface-area-to-	Difficulties in fabrication and repeatability; High cost	Detection of partial discharge (PD)

	volume ratio; Quick response time; Low weight		
Moisture Absorbing Material	Low cost; Low weight; High selectivity to water vapor	Vulnerable to friction; Potential irreversibility in high humidity	Humidity monitoring
Optical Methods	High sensitivity, selectivity and stability; Long lifetime; Insensitive to environment change	Difficulty in miniaturization; High cost	Remote air quality monitoring; Gas leak detection systems with high accuracy ; High-end market applications
Calorimetric Methods	Stable at ambient temperature; Low cost; Adequate sensitivity for industrial detection (ppth range).	Risk of catalyst poisoning and explosion; Intrinsic deficiencies in selectivity	Most combustible gases under industrial environment; Petrochemical plants; Mine tunnels; Kitchens
Gas	Excellent separation	High cost; Difficulty in	Typical laboratory

Chromatograph	performance; High sensitivity and selectivity	miniaturization for portable applications	analysis.
Acoustic Methods	Long lifetime; Avoiding secondary pollution	Low sensitivity; Sensitive to environmental change	Components of Wireless Sensor Networks.

1.2. Performance Parameters of Sensors

Commonly used sensor performance characteristics are listed and defined below.

- **Sensitivity**: is defined as the slope of a calibration curve or change in unit sensor response with change in unit analyte concentration [33]. Different applications need different sensitivity levels, e.g. trace explosives have very low vapor pressures thus small number of molecules can be collected. So, their sensors need to be extremely high sensitive [33].
- **Limit of detection (LOD)** : lowest analyte concentration value that can be detected [33].
- **Resolution**: Smallest concentration variation that can be detected when the concentration is continuously changed [33].

- **Dynamic range**: The analyte concentration from LOD to maximum concentration that can be reliably detected [33].
- **Selectivity**: the ability to detect a specific analyte in the presence of other interfering molecules [33].
- **Reversibility:** The ability of the sensor to return back to its original value when the analyte is removed [33].
- **Response time:** the time required to respond from zero analyte concentration to a step in the concentration [33].
- **Linearity:** The range where the sensor response is in direct proportion to the analyte concentration [33].
- **Hysteresis:** The difference in sensor characteristics for increasing and decreasing analyte concentration [33].

Sensitivity and selectivity are the two most important parameters in designing and applying sensors. For some gases like trace explosives or toxic gases the sensitivity should be extremely high to give signal before the concentration of dangerous/hazardous gases reach a dangerous value. Also, sensors' target gases are not always pure and usually are mixed with other gases. Thus, high selectivity is crucial to have an acceptable rate of false to positives [1], [33].

1.2.1. Sensitivity Improvement Approaches

Several factors affect the sensitivity of a gas sensing method. Amongst all the parameters there are some potential factors that can be manipulated to reach certain level of sensitivity such as chemical component of sensing materials, physical structure of sensing layers, humidity and temperature of the environment [1].

As was mentioned in section 1.1, for some metal oxide semiconductor-based gas sensors temperature variation plays a key role in sensitivity. For example, the working temperature for SnO_2 varies from 25ºC to 500ºC with the optimal sensing temperature of 400ºC for CH_4. If the sensor is designed for sensing more than one gas simultaneously, then the sensitivity should be enhanced for all gases. To ensure the sensitivity of sensor, a thermostatic cycle should be used since different gases have different optimal sensing temperatures. The resistivity of the sensing element is measured during each gas period in the thermostatic cycle. Heating is done by the heating filament built into the sensor [34] . Since there is more than one optimal temperature in the gas mixture, sensors using the thermostatic cycles are equipped with coolers as well in order to turn the value of temperature to the lower one instantly [1].

Gas sensing for molecules that have very low vapor pressures is challenging for relatively small number of molecules can be collected on the surface of sensor. Therefore, pre-concentrators are essential for detection of such gases. Pre-concentrators can improve the detection level significantly by acting as front-end detectors. Pre-concentrating involves three stages: absorption, desorption and conditioning. Typically, a large volume of air, which has very low concentration of target gas, is pumped into the pre-concentrator for a specific period of time, and the target gas and particulate are trapped using the special material. The trapping mechanism is based on adsorption phenomena on large-area surfaces. Then, the adsorption material is heated to a specific temperature to desorb the trapped gas. Conditioning period refers to cooling of the tube to room temperature for the next cycle [1], [33].

Sensitivity can also be enhanced by methods based on other properties rather than electrical ones. One of these methods is photo acoustic spectroscopy (PAS) which is a combination of optics and acoustics. PAS is used for sensing of trace gases via adsorption of appropriate wavelength of infrared or light radiation by the gas molecules inside a photo acoustic cell. An acoustic wave is generated due to the

increased gas temperature inside the cell and pressure rise, which are caused by absorption of modulated light by the molecules. The amplitude of generated acoustic wave is directly proportional to the gas concentration. This amplitude can be detected using a sensitive microphone such as optical cantilever if the laser beam is modulated in the audio frequency range [35].

1.2.2. Selectivity Improvement Approaches

Cross-sensitivity which can be defined as response of sensor to multiple analytes, not necessarily unique, is a common problem for gas sensors which is caused by poor selectivity [1].

Conventional approaches use the “lock-and-key” design in which a specific receptor is used to strongly and highly selectively bind the analyte of interest. In this method, selectivity is achieved via recognition of analyte at the receptor. Relatively, another approach involves using a general physiochemical effect toward a single analyte. In this approach the method of detection determines the species to be sensed. These approaches are only useful when the background and interferences are controlled [36].

Selectivity improving approaches can be classified into two categories:

(1) using sensor arrays, (2) utilizing the difference between optimal conditions for target analytes.

From the two approaches mentioned above, the first one is the main method that can address selectivity issue. Although in the array method the "lock and key" condition of conventional traditional sensors is abandoned, however an array of different sensors which has different cross-sensitive sensing elements is introduce to the system. Each individual element in the array should not necessarily be highly selective toward any given analyte, whereas the collection of individual elements should have as much chemical diversity as possible. In this configuration, identification of an analyte is accomplished through a distinct pattern that is produced by all the sensors in the array and not by the response of each individual sensor [36]. Sensor arrays can help reducing the effects of environment such as temperature and humidity. Furthermore, they can be extended into RFID fields as well.

The sensing elements in the array method can also operate with different sensing principles. For example an array consisted of three

mass sensitive, calorimetric and capacitive transducer can provide a more distinct signature in the multidimensional space. The mass sensitive transducer monitors the shift in the resonance frequency caused by absorption of analytes while the calorimetric one detects enthalpy changes through absorption or desorption of analyte molecules. Also the capacitive transducer can measure the dielectric constant change of the polymer coated as the receptor onto the sensor upon absorption of analytes into the polymer matrix as shown by Hagleitner et. al [37].

Fundamental requirements that should be considered in sensor arrays are [1]:

1. Sensors should be functionally stable and reliable;
2. Sensors should be cross-sensitive to some extent which helps reducing the amount of sensors and increases the array efficiency;
3. The detection efficiency should be high, meaning that the response and recovery time to be short.

The second approach that can be used to address selectivity issue which is utilizing the difference between optimal conditions for target

analytes is a pretty straight forward method. In this method, optimal conditions for the target gas is provided through controlling the actual environment or by compensation and offset, so that to attain the best sensitivity for the target gas and worsening the sensitivity of other gases. Pre-concentrators - if only target gas is concentrated selectively- can be used to enhance the selectivity. Also thermostatic cycle can be utilized to improve selectivity for gases which poses distinct sensing temperatures [1].

Table 3 summarizes the approaches addressed in section 1.2.1. and 1.2.2. for improving selectivity and sensitivity.

Table 1.3: Summary of approaches improving selectivity and sensitivity [1]

Approach	**For Sensitivity**	**For selectivity**
Thermostatic cycle	i. guarantee the best sensitivity of all target gases in each gas period ii. for gases with quite different sensing temperature	i. guarantee the best selectivity of all target gases in each gas period ii. for gases with quite different sensing temperature

Pre-concentrator	i. relative concentration of target gases is improved	i. if pre-concentrator is selective
Photo-acoustic spectroscopy	i. combine advantages of both optic and acoustic methods	N/A
Sensor Array	N/A	i. provide with multi-dimensional signatures ii. for gases with different sensing conditions, the difference is either large or small

1.3. Methane Sensors

1.3.1. Metal Oxide Semi-conductors

The most common semi-conducting metal oxide used toward methane detection is tin oxide (SnO_2) [3], [38]–[40]. SnO_2 is a wide gap semi-conductor which has an n-type electrical conductance due to nonstoichiometric composition resulted by oxygen deficiency. The surface reaction between methane and absorbed oxygen enables it to

sense methane. The sensing mechanism involves chemisorption of oxygen on the surface followed by oxidation of methane with adsorbed oxygen which yields to production of CO_2 and H_2. The conductance of the material will increase as a result of oxygen consumption in the latter reaction [40]. Figure 1 shows the schematic of methane sensing mechanism using SnO_2.

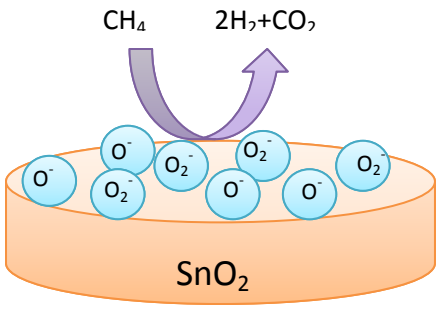

Figure 1.1 Schematic of methane sensing mechanism using SnO2

Bare or untreated SnO_2 has selectivity issues. In order to overcome this problem, noble metal catalyst or dopants such as Pd, Pt, Rh are added to the tin oxide [3], [40]. Other materials such as $BaSnO_3$, $CaZrO_3/MgO$, Ga_2O_3 have also been investigated to address the selectivity issues of tin oxide [4],[3], [40].

There are two major drawbacks associated with metal oxides. One is that they need high temperature in order to achieve the desired sensitivity and the other one is the requirement of presence of oxygen which limits the use of such sensors in anaerobic conditions [40].

1.3.2. Carbon Nanomaterials

The affinity of methane to noble metals has recently been coupled with carbon nanomaterials. Lu et al. [19] reported using single walled carbon nanotubes loaded with palladium (Pd) nanoparticles for detection of methane at room temperature. In this case, Pd nanoparticles attract electrons from the carbon nanotubes followed by adsorption of methane on the Pd. Hence, the current increases through the p-type CNT.

Li et al. [41] have used multi-walled CNTs for room temperature methane detection and similarly have reported the same mechanism proposed by Lu et al. Also, Pal et al.[20] reported using CNTs and Carbon nanofibers (CNFs) alone for detection of methane. However, their study was not confirmed by other groups trying to detect methane with CNTs alone at room temperature.

Other carbon nanomaterials like graphene nanosheets along with conductive polymers have been used toward methane detection as well. Wu et al. [42]reported synthesis and application of graphene nanosheets (graphene)/polyaniline (PANI) nanocomposites as methane sensor.

1.3.3. Optical sensors

Optical detection systems [43]–[47] have also attracted interest for methane detection due to advantages such as ability to operate in a zero-oxygen environment, ability to detect a small amount of gas by choosing appropriate wavelength and intrinsic safety [43]. Stewart et al. [45] have reported the design of a multi-point fiber optic methane sensor using a DFB laser source with a branched fiber network and micro-optic cells. Cong et al. [46] have demonstrated using InGaAsP distributed feedback laser for developing a methane detection system. Massie et al. [44] have designed a sensor based on use of near-IR LEDs operating around the overtone absorption lines of methane at 1660 nm.

1.3.4. Pellistors

Pellistor is a calorimetric combustible gas sensor that consists of a wire coil embedded within a refractory bead loaded with a metal catalyst that is usually Pd [40]. Methane can be oxidized by palladium at 400°C [48] or at platinum surface at around 700°C [49], thus by use of a reference sensor and observing the difference between the electrodes, concentration of methane can be determined [40].

1.3.5. Gas Chromatography

Gas chromatography for methane detection have been utilized in a number of applications including environmental/effluent water, bore holes, human breath, paddy soils and ambient air [40]. Separation capabilities of GC in complex media provides a significant advantage for differentiating between different hydrocarbons [40].

1.4 References

[1] X. Liu, S. Cheng, H. Liu, S. Hu, D. Zhang, and H. Ning, "A survey on gas sensing technology.," *Sensors (Basel).*, vol. 12, no. 7, pp. 9635–65, Jan. 2012.

[2] Y.-F. Sun, S.-B. Liu, F.-L. Meng, J.-Y. Liu, Z. Jin, L.-T. Kong, and J.-H. Liu, "Metal oxide nanostructures and their gas sensing properties: a review.," *Sensors (Basel).*, vol. 12, no. 3, pp. 2610–31, Jan. 2012.

[3] S. Basu and P. K. Basu, "Nanocrystalline Metal Oxides for Methane Sensors: Role of Noble Metals," *J. Sensors*, vol. 2009, pp. 1–20, 2009.

[4] C. Wang, L. Yin, L. Zhang, D. Xiang, and R. Gao, "Metal oxide gas sensors: sensitivity and influencing factors.," *Sensors (Basel).*, vol. 10, no. 3, pp. 2088–106, Jan. 2010.

[5] S. M. Kanan, O. M. El-Kadri, I. A. Abu-Yousef, and M. C. Kanan, "Semiconducting metal oxide based sensors for selective gas pollutant detection.," *Sensors (Basel).*, vol. 9, no. 10, pp. 8158–96, Jan. 2009.

[6] B. C. V. A. I. S. Canada, "Selectivity in semiconductor gas sensors*," vol. 12, pp. 425–440, 1987.

[7] T. A. Emadi, C. Shafai, M. S. Freund, D. J. Thomson, D. S. Jayas, and N. D. G. White, "Development of a Polymer-based Gas Sensor - Humidity and CO 2 Sensitivity," pp. 112–115, 2009.

[8] Z. Wu, X. Chen, S. Zhu, Y. Yao, and H. Guo, "Effect of humidity on electrical properties of micro/nano-polyaniline thin films with different D-CSA doping degree," *Measurement*, vol. 46, no. 1, pp. 411–419, Jan. 2013.

[9] N. T. Tung, T. Khai, M. Jeon, Y. J. Lee, H. Chung, J.-H. Bang, and D. Sohn, "Preparation and characterization of

nanocomposite based on polyaniline and graphene nanosheets," *Macromol. Res.*, vol. 19, no. 2, pp. 203–208, Feb. 2011.

[10] L. D. Tran, D. T. Nguyen, B. H. Nguyen, Q. P. Do, and H. Le Nguyen, "Development of interdigitated arrays coated with functional polyaniline/MWCNT for electrochemical biodetection: application for human papilloma virus.," *Talanta*, vol. 85, no. 3, pp. 1560–5, Sep. 2011.

[11] Q. Lin, Y. Li, and M. Yang, "Polyaniline nanofiber humidity sensor prepared by electrospinning," *Sensors Actuators B Chem.*, vol. 161, no. 1, pp. 967–972, Jan. 2012.

[12] D. Du, X. Ye, J. Cai, J. Liu, and A. Zhang, "Acetylcholinesterase biosensor design based on carbon nanotube-encapsulated polypyrrole and polyaniline copolymer for amperometric detection of organophosphates.," *Biosens. Bioelectron.*, vol. 25, no. 11, pp. 2503–8, Jul. 2010.

[13] B. Adhikari and S. Majumdar, "Polymers in sensor applications," *Prog. Polym. Sci.*, vol. 29, no. 7, pp. 699–766, Jul. 2004.

[14] E. O. Sunden, T. L. Wright, J. Lee, W. P. King, and S. Graham, "Room-temperature chemical vapor deposition and mass detection on a heated atomic force microscope cantilever," *Appl. Phys. Lett.*, vol. 88, no. 3, p. 033107, 2006.

[15] Y. Ando, X. Zhao, T. Sugai, and M. Kumar, "carbon nanotubes," no. October, pp. 22–29, 2004.

[16] M. H. Ervin, B. S. Miller, B. Hanrahan, B. Mailly, and T. Palacios, "A comparison of single-wall carbon nanotube electrochemical capacitor electrode fabrication methods," *Electrochim. Acta*, vol. 65, pp. 37–43, Mar. 2012.

[17] E. Llobet, "Gas sensors using carbon nanomaterials: A review," *Sensors Actuators B Chem.*, vol. 179, pp. 32–45, Mar. 2013.

[18] M. Cano, A. M. Benito, W. K. Maser, and E. P. Urriolabeitia, "Formation of multiwalled carbon nanotube-Pd nanoparticle

nanocomposites : influence of the reaction media and applications on catalyzed C-C coupling," pp. 2–3.

[19] Y. Lu, J. Li, J. Han, H.-T. Ng, C. Binder, C. Partridge, and M. Meyyappan, "Room temperature methane detection using palladium loaded single-walled carbon nanotube sensors," *Chem. Phys. Lett.*, vol. 391, no. 4–6, pp. 344–348, Jun. 2004.

[20] R. K. Roy, M. P. Chowdhury, and a. K. Pal, "Room temperature sensor based on carbon nanotubes and nanofibres for methane detection," *Vacuum*, vol. 77, no. 3, pp. 223–229, Feb. 2005.

[21] D. R. Kauffman and A. Star, "Carbon nanotube gas and vapor sensors.," *Angew. Chem. Int. Ed. Engl.*, vol. 47, no. 35, pp. 6550–70, Jan. 2008.

[22] J. Huang, D. Wang, H. Hou, and T. You, "Electrospun Palladium Nanoparticle-Loaded Carbon Nanofibers and Their Electrocatalytic Activities towards Hydrogen Peroxide and NADH," *Adv. Funct. Mater.*, vol. 18, no. 3, pp. 441–448, Feb. 2008.

[23] M. Penza, G. Cassano, R. Rossi, M. Alvisi, a. Rizzo, M. a. Signore, T. Dikonimos, E. Serra, and R. Giorgi, "Enhancement of sensitivity in gas chemiresistors based on carbon nanotube surface functionalized with noble metal (Au, Pt) nanoclusters," *Appl. Phys. Lett.*, vol. 90, no. 17, p. 173123, 2007.

[24] C. Staii, A. T. Johnson, M. Chen, and A. Gelperin, "DNA-decorated carbon nanotubes for chemical sensing.," *Nano Lett.*, vol. 5, no. 9, pp. 1774–8, Sep. 2005.

[25] F. Schedin, a K. Geim, S. V Morozov, E. W. Hill, P. Blake, M. I. Katsnelson, and K. S. Novoselov, "Detection of individual gas molecules adsorbed on graphene.," *Nat. Mater.*, vol. 6, no. 9, pp. 652–5, Sep. 2007.

[26] A. Elia, C. Di Franco, G. Scamarcio, and V. Amendola, "Photoacoustic Spectroscopy with Quantum Cascade Lasers for Trace Gas Detection," pp. 1411–1419, 2006.

[27] http://www.e2v.com/e2v/assets/File/sensors_datashe.

[28] http://chem.wisc.edu/deptfiles/genchem/lab/labdocs.

[29] http://teaching.shu.ac.uk/hwb/chemistry/tutorials/.

[30] S. Minglei, L. Xiang, Z. Changping, and Z. Jiahua, "Gas concentration detection using ultrasonic based on wireless sensor networks," *2nd Int. Conf. Inf. Sci. Eng.*, vol. C, no. 1, pp. 2101–2106, Dec. 2010.

[31] M. Sonoyama, Y. Kato, and H. Fujita, "Application of ultrasonic to a hydrogen sensor," *2010 IEEE Sensors*, no. 3, pp. 2141–2144, Nov. 2010.

[32] E. Nv and S. Jacobson, "New Developments in Ultrasonic Gas Analysis and Flowmetering," pp. 508–516, 2008.

[33] L. Senesac and T. G. Thundat, "Nanosensors for trace," vol. 11, no. 3, pp. 28–36, 2008.

[34] E. Cordos, L. Ferenczi, S. Cadar, S. Costiug, G. Pitl, A. Aciu, and A. Ghita, "Methane and Carbon Monoxide Gas Detection system based on semiconductor sensor," *2006 IEEE Int. Conf. Autom. Qual. Testing, Robot.*, vol. 2, pp. 208–211, May 2006.

[35] A. Elia, C. Di Franco, G. Scamarcio, and V. Amendola, "Photoacoustic Spectroscopy with Quantum Cascade Lasers for Trace Gas Detection," pp. 1411–1419, 2006.

[36] K. J. Albert, N. S. Lewis, C. L. Schauer, G. a Sotzing, S. E. Stitzel, T. P. Vaid, and D. R. Walt, "Cross-reactive chemical sensor arrays.," *Chem. Rev.*, vol. 100, no. 7, pp. 2595–626, Jul. 2000.

[37] C. Capacitive, M. Microsensors, C. Hagleitner, S. Member, D. Lange, A. Hierlemann, O. Brand, A. Member, H. Baltes, and S. Member, "CMOS Single-Chip Gas Detection System," vol. 37, no. 12, pp. 1867–1878, 2002.

[38] a Biaggi-Labiosa, F. Solá, M. Lebrón-Colón, L. J. Evans, J. C. Xu, G. Hunter, G. M. Berger, and J. M. González, "A novel methane sensor based on porous SnO2 nanorods: room temperature to high temperature detection.," *Nanotechnology*, vol. 23, no. 45, p. 455501, Nov. 2012.

[39] F. Quaranta, R. Rella, P. Siciliano, S. Capone, M. Epifani, and L. Vasanelli, "A novel gas sensor based on SnO 2 r Os thin film for the detection of methane at low temperature," pp. 350–355, 1999.

[40] N. S. Lawrence, "Analytical detection methodologies for methane and related hydrocarbons.," *Talanta*, vol. 69, no. 2, pp. 385–92, Apr. 2006.

[41] Y. Li, H. Wang, Y. Chen, and M. Yang, "A multi-walled carbon nanotube/palladium nanocomposite prepared by a facile method for the detection of methane at room temperature," *Sensors Actuators B Chem.*, vol. 132, no. 1, pp. 155–158, May 2008.

[42] Z. Wu, X. Chen, S. Zhu, Z. Zhou, Y. Yao, W. Quan, and B. Liu, "Room Temperature Methane Sensor Based on Graphene Nanosheets / Polyaniline Nanocomposite Thin Film," vol. 13, no. 2, pp. 777–782, 2013.

[43] C. Chen, R. W. Newcomb, and Y. Wang, "A trace methane gas sensor using mid-infrared quantum cascaded laser at 7.5 μm," *Appl. Phys. B*, vol. 113, no. 4, pp. 491–501, May 2013.

[44] C. Massie, G. Stewart, G. McGregor, and J. R. Gilchrist, "Design of a portable optical sensor for methane gas detection," *Sensors Actuators B Chem.*, vol. 113, no. 2, pp. 830–836, Feb. 2006.

[45] G. Stewart, C. Tandy, D. Moodie, M. A. Morante, and F. Dong, "Design of a fibre optic multi-point sensor for gas detection," *Sensors Actuators B Chem.*, vol. 51, no. 1–3, pp. 227–232, Aug. 1998.

[46] M. E. Cong, S. H. Guo, and Y. I. Wang, “A novel methane detection system based on InGaAsP distributed feedback laser,” *Int. J. Opt. Appl.*, vol. XLI, no. 3, pp. 639–648, 2011.

[47] O. Hennig, R. Strzoda, E. Mágori, E. Chemisky, C. Tump, M. Fleischer, H. Meixner, and I. Eisele, “Hand-held unit for simultaneous detection of methane and ethane based on NIR-absorption spectroscopy,” *Sensors Actuators B Chem.*, vol. 95, no. 1–3, pp. 151–156, Oct. 2003.

[48] E. M. Logothetis, M. D. Hurley, W. J. Kaiser, and Y. C. Yao, “in proceedings 2nd International Meeting on Chemical Sensors : Bordeaux, France, 1986,” in *2nd International Meeting on Chemical Sensors : Bordeaux, France,*, 1986, p. 175.

[49] H. Debeda, L. Dulau, P. Dondon, F. Menil, C. Lucat, and P. Massok, “Development of a reliable methane detector,” *Sensors Actuators B Chem.*, vol. 44, no. 1–3, pp. 248–256, Oct. 1997.

Chapter 2: Room Temperature Detection of Methane Using Photothermal Cantilever Deflection Spectroscopy

2.1. Introduction

Methane (CH4), the main constituent of natural gas, is a colorless, highly volatile odorless flammable gas [1] that can cause explosion at concentrations between 5-15 V/V % due to its ready flammability [2]. Thus, developing a reliable, yet cost effective methane sensor is of great interest concern especially for safe operations in coal mines and factories [3]. However, detection of methane at room temperature is still a challenge due to the inert property of methane, which is non polar and shows little tendency to lose or gain electrons at room temperature [4]. Therefore, detection approaches based on chemoselective interfaces are not very effective in relatively inert molecules such as methane. Optical detection systems [5]–[9] for methane detection have attracted attention due to their advantages such as ability to operate in a zero-oxygen environment, ability to detect a small amount of gas by choosing appropriate wavelength and as well as intrinsic safety of the detection system [5]. Stewart et al. [7] have reported the design of a multi-point fiber optic methane sensor using a DFB laser source with a branched fiber network and micro-

optic cells. Cong et al. [8] have demonstrated using InGaAsP distributed feedback laser for developing a methane detection system. Massie et al. [6] have designed a sensor based on use of near-IR LEDs operating around the overtone absorption lines of methane at 1660 nm. The spectrum in the mid infrared (IR) region, however, provides "molecular finger print "due to the uniqueness of molecular vibration in the mid infrared that is free over overtones. Though highly selective, IR spectroscopy is not very sensitive in mid-IR region [10], [11].

Photothermal cantilever deflection spectroscopy (PCDS) combines the extreme thermal sensitivity of a bi-metallic microcantilever with the high selectivity of mid-IR. This technique enables obtaining molecular signature of trace amount of adsorbed molecules on the cantilever surface [11]–[14]. In this technique, the target molecules are first adsorbed on the bimetallic cantilever. During resonant excitation of adsorbed molecules with IR light, the cantilever undergoes deflection due to heat generated due to non-radiative decay. The amplitude of cantilever deflection as a function of IR wavelength closely resembles the IR absorption peaks of the molecules. Unlike the detectors used in conventional IR absorption spectroscopy, which

requires cooled mid-IR detectors, the bimetallic cantilever is uncooled and has temperature sensitivity in 10mK range. Unlike conventional photon detection based sensing, detection of optical absorption using thermal effects offers a higher signal-to-noise ratio, which increases with incident photon intensity. Therefore, by using recent advances in high brightness mid infrared light sources such as quantum cascade lasers (QCL) it is possible to detect extremely small amount of materials [11].

Here, we report on detecting femtogram level adsorbed molecules on a cantilever using photothermal cantilever deflection spectroscopy. Methane molecules as physisorbed on the bimetallic cantilever, which eliminate the need for using any chemoselective interface for detection or even using as a pre-concentrator to increase the number of molecules adsorbed on the cantilever. Using kinetic theory of gases we have estimated the resident time of the methane molecules on the cantilever as 0.1 nano seconds. Therefore, at any moment there must be a small fraction of methane molecules adsorbed on the surface long enough to transfer their vibrational energy to the cantilever as heat. Unlike chemoselective interface-based microsensors in which

operation life is shortened by degradation of coating, PCDS technique offers a robust, selective and sensitive single microstructure without using of any chemoselective interface [11].

2.1.1. IR Spectroscopy Principles

Infrared spectroscopy provides detailed information on the chemical composition at the molecular level. When a material is exposed to IR radiation, the adsorbed radiation excites molecules to higher vibrational state. The wavelengths absorbed by the material are characteristics of its molecular structure. This technique can also investigate sample compositions and mixtures as well. The basic principal of IR method is based on the fact that chemical bonds or groups of bonds vibrate at characteristic frequencies. Molecules exposed to IR radiation of certain wavelength resonantly absorb the energy at frequencies that are characteristics of that molecule. It should be noted that only molecules which have a dipole moment can be IR active. In the other words, IR spectroscopy detects changes in the dipole moment of molecules. FT-IR spectroscopy is also categorized in vibrational spectroscopy techniques. Like IR spectroscopy, when a material is put into FT-IR spectrometer, it

absorbs the radiation emitted and the absorption displays the molecular finger print of the material being investigated [15].

2.1.2. Beer-Lambert Law

Beer-Lambert law relates the absorption of light to the properties of the material through which the light is traveling. It states that the dependence of transmission of light T through the substance and the product of the distance l that light travels through the material and the absorption coefficient α of substance, is logarithmic[16].

$$T = \frac{I}{I_0} = e^{-\alpha l} \qquad (2.1)$$

2.2. Experimental

2.2.1. Microcantilever preparation

We have used commercially available rectangular silicon cantilevers (OCTO 500-D, Micromotive, Germany) for these experiments. The dimensions of the cantilevers used in this study were 450 μm in length, 90 μm in width and 1 μm in thickness. The cantilevers were cleaned by rinsing with acetone, ethanol and UV ozone treatment prior to coating with gold. Gold coating was carried out using an e-beam evaporator. A thin layer of chromium (10 nm) used as an

adhesion layer for the 200 nm of gold. Prior to the measurements, each cantilever was again rinsed with acetone and ethanol and dried in the vacuum oven.

2.2.2. PCDS experimental setup

The PCDS setup used in this study is shown in Fig. 2.1. The microcantilever was mounted on a cantilever holder attached to the Multimode atomic force microscope (AFM) head (Bruker, Santa Barbara, CA). The monochromator used as an IR source (Foxboro Miran 1A-CVF) was mechanically chopped at 80 Hz and focused on the cantilever. The IR wavelength was then scanned from 2.5 microns to 14.5 microns (4000 cm^{-1} to 690 cm^{-1} in wavenumber) with a resolution of 0.05 μm at 3 μm, 0.12 μm at 6 μm and 0.25 μm at 11 μm according to the manufacturer. For some experiments we also used Quantum Cascade Laser (QCL) (Daylight Solutions, UT-8). The QCL operated at 200 KHz pulse rate with 10% duty cycle and was modulated at 80 Hz using DS345 function generator (Stanford Research System, Sunnyvale, CA). The IR wavelength was scanned from 7.1 μm to 8.3 μm (1408 cm^{-1} to 1204 cm^{-1} in wavenumber) with spectral resolution of 5 nm. The nanomechanical IR spectrum was

taken using a SR850 lock-in amplifier (Stanford Research System, Sunnyvale, CA) and the resonance frequency of the microcantilevers was measured with SR760 spectrum analyzer (Stanford Research System, Sunnyvale, CA). A custom-developed Lab View software was used for data acquisition and data processing.

2.2.3. Gas sensing

Gas sensing measurements were conducted in an air tight test chamber with an IR window which was mounted on the cantilever holder and had gas injection ports. Gas flow was regulated by mass flow controllers (MFCs) (Cole-Parmer®), which were programmed and controlled remotely by a computer. A typical gas sensing cycle consisted of three sequential steps, i.e.; (1) baseline recording – exposing cantilever to dry N_2 and obtaining the spectrum; (2) sensing-switching from dry N_2 to the target gas, methane (2.5 % vol balanced with N_2 from Praxair®), and obtaining the spectrum; (3) recovery-switching off the target gas and re-exposing the cantilever to dry N_2 . Each cycle was repeated three times for a specific concentration. The detection limit test was done in a similar fashion except that the target gas was diluted into different concentrations with dry N_2. Computer

controlled MFCs gave a continuous gas flow at a rate of 300 standard cubic centimeters per minute (sccm)

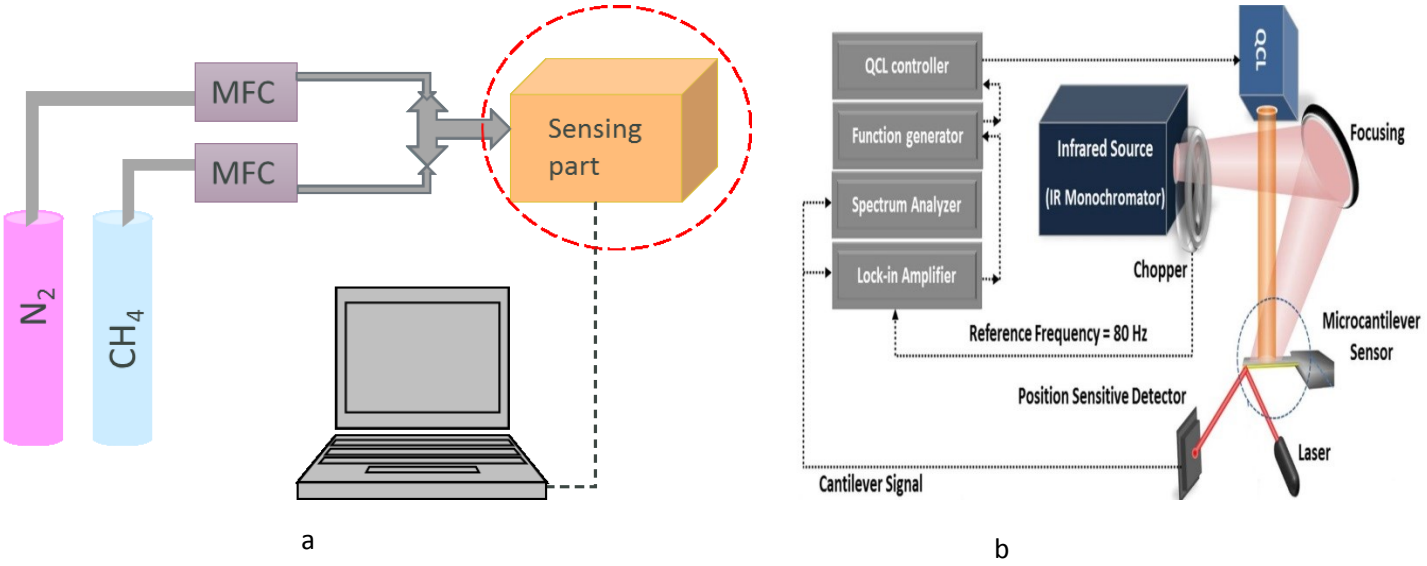

Figure 2.1 Schematic drawing of the gas sensing setup consisted of PCDS. a) gas sensing setup b)sensing part (picture from reference [11])

2.3. Results and Discussion

2.3.1. Nanomechanical IR absorption spectrum

The nanomechanical IR spectrum of different concentrations of methane is shown in Fig. 2.2. Each spectrum is an average of three different scans. There are several distinct peaks around the highest peak at 7660 nm, which are in good agreement with methane spectrum obtained from National Institute of Standards and Technology (NIST). However, the highest peak which is at 7660 nm

was considered as the reference for this work. Since mixtures with higher concentration of methane had peaks with higher intensity compared to lower concentration mixtures, they are plotted in a different graph for clarity. It was noted that the main peak at 7660 nm had a slight shift of about 10 nm for concentrations lower than 0.25 vol%. Figure 2.3 shows the amplitude of cantilever deflection for different concentrations of methane at 7660 nm. It is observed that the intensity of the peak has an almost linear relation with concentration of absorbed gas on the surface of the cantilever.

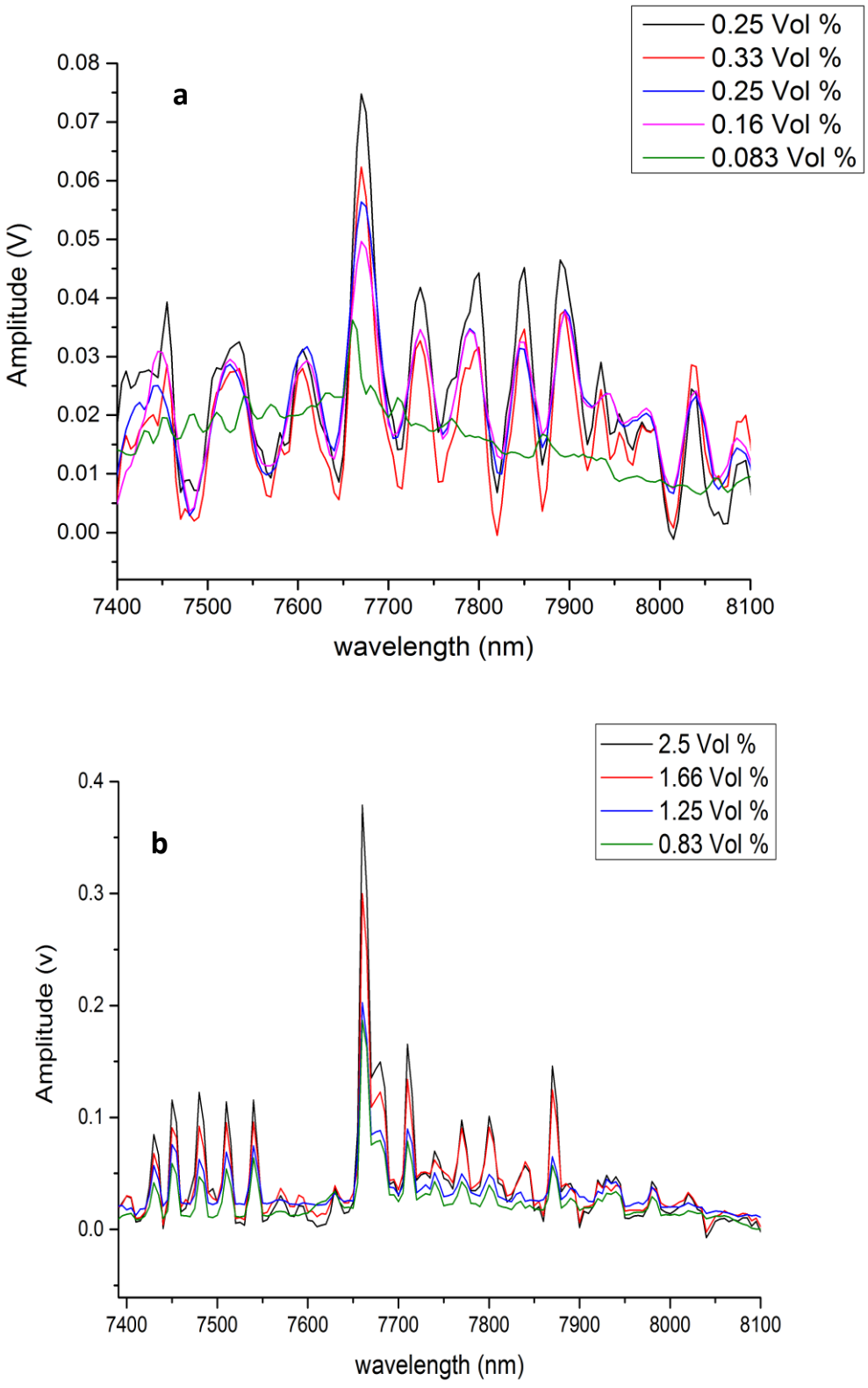

Figure 2.2 PCDS spectrum of methane. a) 0.083-0.25 Vol % b) 0.83-2.5 Vol%

The peaks obtained with PCDS show different relative intensities in the PCDS spectrum compared to the conventional FTIR spectrum. The observed difference is mainly due to the different fundamental mechanism involved in the detection process. Conventional IR detection is based on Beer–Lambert principle which depends on the ratio of the intensities of scattered (or transmitted) photon intensity and the incident photon whereas the PCDS relies on the heat generated during absorption process and does not detect photons. Thus, depending on the relaxation process the PCDS and the conventional IR absorption peak intensities can be different [11], [17]. However, the peak position (wavelength) shows an excellent agreement between the PCDS and the conventional techniques.

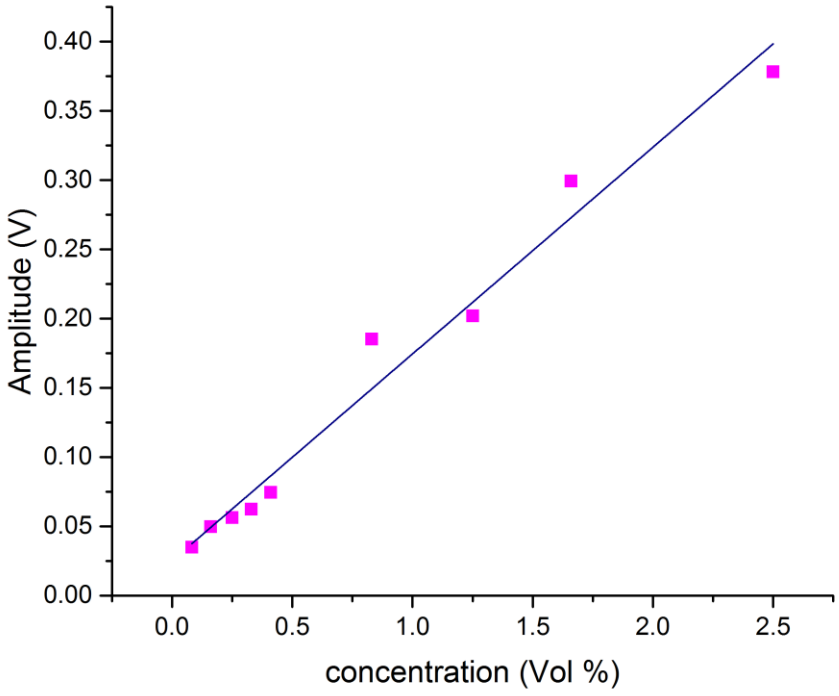

Figure 2.3 The peak amplitude at 7660 nm as a function of concentration

2.3.2. Adsorbed mass and residence time of methane

Fundamental resonance frequency f_0 of a microcantilever in the absence of damping can be calculated as [18]

$$f_0 = \frac{1}{2\pi}\sqrt{\frac{k}{m_0}} \quad (2.2a)$$

Where k is the spring constant of the cantilever and m_0 is the effective suspended mass. Equation (*2.2a*) gives a good approximation of resonance frequency for weakly damped resonators

such as microscopic cantilever in the air. It is reasonable to assume that spring constant remains unaffected when equation (*2.2a*) is used for analysis of gravimetric response of a microcantilever. Therefore, the changes in the mass Δm can be calculated as

$$\Delta m = \frac{k}{4\pi^2}\left(\frac{1}{f_1^2} - \frac{1}{f_0^2}\right) \quad (2.2b)$$

Where f_0 and f_1 are the resonance frequency before and following molecular adsorption [18].

The resonance frequency change gives real time information about the absorbed mass on the microcantilever. However, in this study the resonance frequency did not show a change due to methane adsorption indicating that the amount of adsorbed gas below the resolution limit of frequency measurement. This is due to inert properties of methane and its extremely small residence time of methane on the cantilever. However, by using kinetic theory of gases the absorbed mass and the residence time of methane can be calculated [19].

If n is the number of molecules striking a unit area of a surface per unit time, and τ is the average time that molecules remain on the surface, then σ number of molecules per unit area of surface can be calculated by:

$$\sigma = n\tau \quad (2.3)$$

Assuming that methane is acting as an ideal gas, then

$$n = \frac{1}{4} N_1 \bar{u} \quad (2.4)$$

Where $\bar{u}$ is mean velocity, N_1 is the number of molecules of the gas per cm^3. By applying other fundamental equations, (2.4) can be rewritten as:

$$p = \frac{1}{3} N_1 m \overline{u^2} \quad (2.5)$$

Where m is mass of a molecule and $\overline{u^2}$ stands for the average of all square of velocities. The relation between $\overline{u^2}$ and $(\bar{u})^2$ follows from Maxwell's law and can be expressed as

$$\frac{1}{3} \overline{u^2} = \frac{1}{8} \pi (\bar{u})^2 \quad (2.6)$$

Substituting (2.6) in (2.5) leads to

$$\bar{u} = \sqrt{\frac{8p}{\pi N_1 m}} \quad (2.7)$$

N_1 is defined as the number of molecules of the gas per cm^3 , hence it can be expressed as

$$N_1 = \frac{N}{V} \quad (2.8)$$

Where N is Avogadro's number and V is the volume of a mole expressed in cm^3. By substituting (2.8) in the equation (2.7), $\bar{u}$ can be obtained as

$$\bar{u} = \sqrt{\frac{8pV}{\pi Nm}} \quad (2.9)$$

Using ideal gas law, $pV = RT$, and realizing that $Nm = M$, where M is molecular weight and R is gas constant, (2.9) can be written as

$$\bar{u} = \sqrt{\frac{8RT}{\pi M}} \quad (2.10)$$

Substituting (2.10) and (2.8) in (2.4), n can be obtained as

$$n = \frac{Np}{\sqrt{2\,\pi\,MRT}} \quad (2.11)$$

2.3.3. Dependence of τ on temperature

The magnitude of τ is greatly dependent on temperature. This might be expected theoretically from the following equation which had been given by Frenkel in 1924 [19].

$$\tau = \tau_0 e^{Q/RT} \quad (2.12)$$

Where is τ_0 the time of oscillation of molecules in the adsorbed state, Q is the heat of adsorption which is defined as the amount of heat transferred when the molecule is absorbed on the surface. It should be noted that τ_0 has no relation to the time of vibration of the constituent molecules or atoms of the adsorbing surface.

It's clear from equation (2.12) that magnitude of τ is also dependent of Q. In fact, heat of adsorption is mainly responsible for the amount of time during which the adsorbed molecules will stay at the surface before leaving it. "*The exact magnitude of the constant* τ_0 *is related to the loss of entropy due to adsorption from gas phase. However, it can be stated that once a molecule has lost exactly one degree of freedom of translation upon adsorption, while retaining at the same time all its degree of freedom of rotation and internal vibration,* τ_0 *may be shown to be equal to* h/kT*, which amounts to* 1.6×10^{-13} *sec. at room temperature*," [19].

2.3.4. Amount of adsorbed methane on the cantilever and residence time

Amount of adsorbed methane on the surface of the cantilever can be calculated from (2.3). Assuming that methane has heat of adsorption equal to 4 kcal/mol on gold surface and τ_0 is equal to 1.6×10^{-13} sec, then

$$\sigma = 1.9 \times 10^{16}\, molecule.m^{-2}$$

The surface area of the cantilever used in this study was 40500 μm^2, thus the absorbed mass of methane on the cantilever should be around $1.8 \times 10^{-14} gr$ and the residence time of adsorbed methane calculated from (2.12) may be 1.1×10^{-10} sec.

Knowing the adsorbed mass of methane, the resonance frequency change of the cantilever as a result of methane exposure can be theoretically calculated using (2.2b). Solving (2.2b) for f_1, shows that the expected resonance frequency change is less than 1 Hz, which is well below the resolution of the setup used for measuring the resonance frequency. Using the concentration of methane in the chamber and the amount that adsorbed on the surface, the average sticking coefficient of methane can be estimated as 10^{-5}.

2.4. Summary

We have demonstrated a nanomechanical IR spectroscopy based sensor with QCL for methane detection without using any chemoselective interface which is fast, selective, sensitive and inexpensive and has a potential of being miniaturized for field applications. By combining the selectivity of mid-IR spectroscopy and sensitivity of a bi-material cantilever, IR absorption spectrum of methane in pico gram quantities was obtained. Also, absorbed mass of methane and residence time was calculated using the kinetic theory of gases.

2.5. References

[1] a Biaggi-Labiosa, F. Solá, M. Lebrón-Colón, L. J. Evans, J. C. Xu, G. Hunter, G. M. Berger, and J. M. González, "A novel methane sensor based on porous SnO2 nanorods: room temperature to high temperature detection.," *Nanotechnology*, vol. 23, no. 45, p. 455501, Nov. 2012.

[2] C. L. Yaws, *Matheson gas data book*, 7th ed. New York: McGraw-Hill, 2001.

[3] G. Xie, P. Sun, X. Yan, X. Du, and Y. Jiang, "Fabrication of methane gas sensor by layer-by-layer self-assembly of polyaniline/PdO ultra thin films on quartz crystal microbalance,"

Sensors Actuators B Chem., vol. 145, no. 1, pp. 373–377, Mar. 2010.

[4] Y. Li, H. Wang, Y. Chen, and M. Yang, "A multi-walled carbon nanotube/palladium nanocomposite prepared by a facile method for the detection of methane at room temperature," *Sensors Actuators B Chem.*, vol. 132, no. 1, pp. 155–158, May 2008.

[5] C. Chen, R. W. Newcomb, and Y. Wang, "A trace methane gas sensor using mid-infrared quantum cascaded laser at 7.5 μm," *Appl. Phys. B*, vol. 113, no. 4, pp. 491–501, May 2013.

[6] C. Massie, G. Stewart, G. McGregor, and J. R. Gilchrist, "Design of a portable optical sensor for methane gas detection," *Sensors Actuators B Chem.*, vol. 113, no. 2, pp. 830–836, Feb. 2006.

[7] G. Stewart, C. Tandy, D. Moodie, M. A. Morante, and F. Dong, "Design of a fibre optic multi-point sensor for gas detection," *Sensors Actuators B Chem.*, vol. 51, no. 1–3, pp. 227–232, Aug. 1998.

[8] M. E. Cong, S. H. Guo, and Y. I. Wang, "A novel methane detection system based on InGaAsP distributed feedback laser," *Int. J. Opt. Appl.*, vol. XLI, no. 3, pp. 639–648, 2011.

[9] O. Hennig, R. Strzoda, E. Mágori, E. Chemisky, C. Tump, M. Fleischer, H. Meixner, and I. Eisele, "Hand-held unit for simultaneous detection of methane and ethane based on NIR-absorption spectroscopy," *Sensors Actuators B Chem.*, vol. 95, no. 1–3, pp. 151–156, Oct. 2003.

[10] S. Kim, D. Lee, R. Thundat, M. Bagheri, S. Jeon, and T. Thundat, "Photothermal Cantilever Deflection Spectroscopy," *ECS Trans.*, vol. 50, no. 12, pp. 459–464, 2012.

[11] S. Kim, D. Lee, X. Liu, C. Van Neste, S. Jeon, and T. Thundat, "Molecular recognition using receptor-free nanomechanical infrared spectroscopy based on a quantum cascade laser," *Sci. Rep.*, pp. 1–6, 2013.

[12] A. R. Krause, C. Van Neste, L. Senesac, T. Thundat, and E. Finot, “Trace explosive detection using photothermal deflection spectroscopy,” *J. Appl. Phys.*, vol. 103, no. 9, p. 094906, 2008.

[13] E. A. Wachter, T. Thundat, P. I. Oden, R. J. Warmack, P. G. Datskos, and S. L. Sharp, “Remote optical detection using microcantilevers,” *Rev. Sci. Instrum.*, vol. 67, no. 10, p. 3434, 1996.

[14] J. R. Barnes, R. J. Stephenson, M. E. Welland, C. Gerber, and J. K. Gimzewski, “Photothermal spectroscopy with femtojoule sensitivity using a micromechanical device,” *Nature*, vol. 372, no. 6501, pp. 79–81, 1994.

[15] S. Rehman, “Introduction to Spectroscopy,” in *Vibrational Spectroscopy in Tissue analysis*, 2012, pp. 8–10.

[16] J. D. Ingle, *Spectrochemical analysis*. Prentice Hall, 1998.

[17] M. Bagheri, I. Chae, D. Lee, S. Kim, and T. Thundat, “Sensors and Actuators B : Chemical Selective detection of physisorbed hydrocarbons using photothermal cantilever deflection spectroscopy,” vol. 191, pp. 765–769, 2014.

[18] N. V. Lavrik, M. J. Sepaniak, and P. G. Datskos, “Cantilever transducers as a platform for chemical and biological sensors,” *Rev. Sci. Instrum.*, vol. 75, no. 7, p. 2229, 2004.

[19] J. H. Boer, *The Dynamical Character Of Adsorpton*, Second Edi. Oxford University Press, 1968.

Chapter 3: Synthesis and application of Pd nanoparticles for room temperature methane detection using palladium loaded single-walled carbon nanotubes

3.1. Introduction

The detection of methane has attracted a lot of concern during the recent years since it is not only considered as a combustible gas at room temperature (5-15 vol% concentration) but also its effect as a greenhouse gas [1]–[5]. One of the methods used toward detection of methane is employing metal oxide semiconductors like tin oxide (SnO_2). As was discussed in chapter one, these sensors have advantages such as low cost and good sensitivity but their working temperature is often as high as 500°C since their working mechanism is based on chemical oxidation or decomposition of methane [2], [6], [7]. Techniques based on laser detection and infrared can detect methane at very low concentrations even at room temperature, however they can be bulky and expensive[1], [8]–[10]. For gas molecules like methane that are inert at room temperature and exhibit very small or no tendency toward electron acceptance or donation, single walled carbon nanotubes (SWCNTs) can be used as gas

sensors. However, they can only be used as gas sensors if they are properly loaded with transition metals such as palladium (Pd) and platinum (Pt). Lu et al.[4] have reported using Pd loaded SWCNTs for methane detection at room temperature via sputtering Pd onto the pile of SWCNTs. Li et al. [1] have prepared a composite of multi-walled carbon nanotube and palladium nanoparticles by reducing their aqueous mixture with $NaBH_4$. Also use of conducting polymers such as polyaniline for room temperature methane detection have been investigated [11].

Here we have demonstrated a microfabricated interdigitated electrode that has been coated with Pd-SWCNTs. The acid treated SWCNTs have been decorated with Pd nanoparticles via chemical reduction of precursor (Pd^{2+}).

3.2. Experimental

3.2.1. Materials

Single walled carbon nanotubes (SWCNT) with purity greater than 95% prepared by CVD method that had the diameter of 1.5 nm and length of 1-5 μm were purchased from NanoLab Inc. (USA). For the purpose of incorporating palladium (Pd) nanoparticles into the SWCTs, 99.99% pure granular Sodium borohydride ($NaBH_4$),

Palladium (II) chloride ($PdCl_2$) with a purity of 99.99%, 7 N Ammonia (NH_3) solution in methanol, 99.99% pure Boric acid (H_3BO_3) and 99.99% pure Ammonium fluoride (NH_4F) were purchased from Sigma Aldrich (Canada).

3.2.2. Methods

3.2.2.1 Purification of SWCNTs

Prior to use, 200 mg of SWCNTs was refluxed in 20 ml of 7 M HNO_3 for 12 hour at 120ºC to remove impurities and create oxygen containing functional groups on the surface of nanotubes [2]. The acid treated SWCNTs were washed thoroughly with DI water, centrifuged and dried under vacuum at room temperature for further use.

3.2.2.2. Synthesis of Pd-SWCNT nanostructure

Pd-SWCNTs were synthesized using modified procedure for preparation of Pd-C (Vulcan XC-72 carbon) catalyst [12]. 25 mg of NH_4F, 125 mg of H_3BO_3 and 3.13 ml of $PdCl_2$ 0.045 M were dissolved into 10 ml of DI water. The mixture was well stirred

followed by addition of 60 mg of acid treated SWCNT and was ultrasonicated in order to get the SWCNTs dispersed. To set the PH of solution to 8-9, a sufficient amount of concentrated NH_3 was used. Once the PH was adjusted, 10 ml of 0.03 M $NaBH_4$ was added dropwise under vigorous stirring. The mixture was then magnetically stirred for another 8 hours in order to complete the reaction. The products were collected using vacuum filter and then rinsed with sufficient water followed by vacuum drying at 60ºC.

3.2.2.3. Characterization of Pd-SWCNT nanostructures

The Pd-SWCNT nanostructures were characterized using Field Emission Scanning Electron Microscopy (FE-SEM, JAMP- 9500F, JEOL, USA) to examine the morphology of nanostructures. All samples for FE-SEM analysis were gold sputtered using a Denton Gold Sputter unit (USA). Tunneling Electron Microscopy (TEM) was utilized to determine Pd nanoparticles size and morphology. To obtain TEM images, the as prepared Pd-SWCNT powder was dispersed in EOH and ultrasonicated for 30 minutes in order to form a homogenous mixture. Then the solution was drop casted on a copper grid and dried at room temperature before TEM investigation.

3.2.2.4. Gas Sensing

Gas sensing measurements were conducted in an air tight flow cell which was designed by SolidWorks software and was 3D printed. The flow cell had gas injection ports along with ports for placing micro heater if heating was needed in any parts of the experiments. Figure 3.1 shows the side view of the as designed flow cell. Gas flow was regulated by mass flow controllers (MFCs) (Cole-Parmer®), which were programmed and controlled remotely by a computer. A typical gas sensing cycle consisted of three sequential steps, i.e.; (1) baseline recording – exposing sensor to dry N_2 and reading the resistance after stabilization; (2) sensing- switching from dry N_2 to the target gas, methane (2.5 % vol balanced with N_2 from Praxair®), and recording the resistance; (3) recovery- switching off the target gas and re-exposing the sensor to dry N_2. Each cycle was repeated three times for a specific concentration. In order to investigate the response of sensor to different concentrations of methane, same tests were done in a similar fashion except that the target gas was diluted into different concentrations with dry N_2. Computer controlled MFCs gave a continuous gas flow at a rate of 300 standard cubic centimeters per minute (sccm).

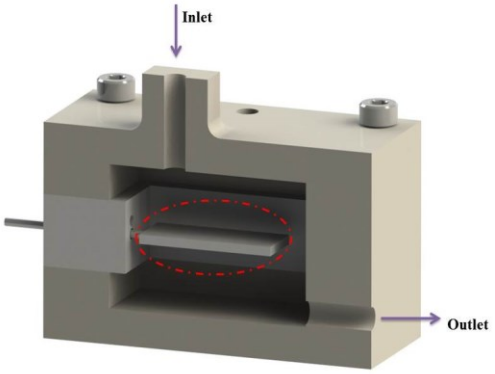

Figure 3.1 3D side view of the flow cell

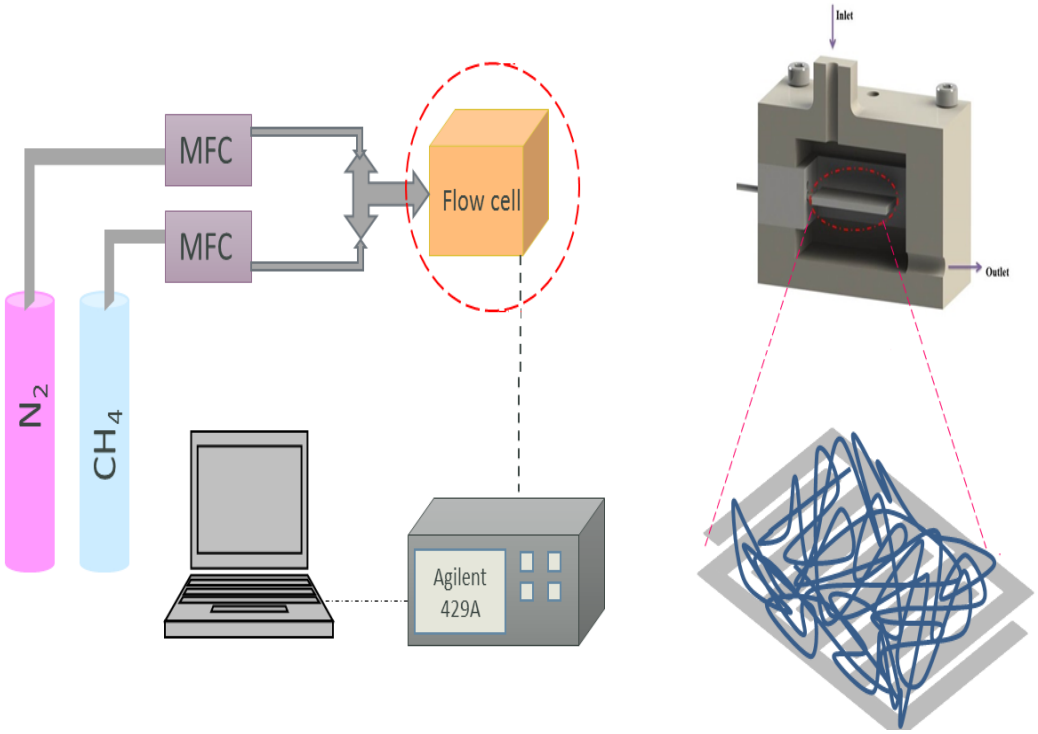

Figure 3.2 Schematic drawing of the experimental setup

3.2.2.5. Sensing platform and fabrication process

The sensing platform used in this study is an integrated electrode (IDE) which consists of two gold electrodes on a glass substrate that are connected by interdigitated fingers. The fabrication process of the sensor was as follow. Fabricated IDEs were washed with acetone and ethanol prior to use to remove any photoresist residue from the fabrication process. The as prepared Pd loaded SWCNTs solution (Pd-SWCNT powder dispersed in ethanol and ultrasonicated to form a homogenous), was then dropcasted onto the interdigitated fingers to create a sensor. Figure 3.3 shows the process of fabrication of the IDE used in this study.

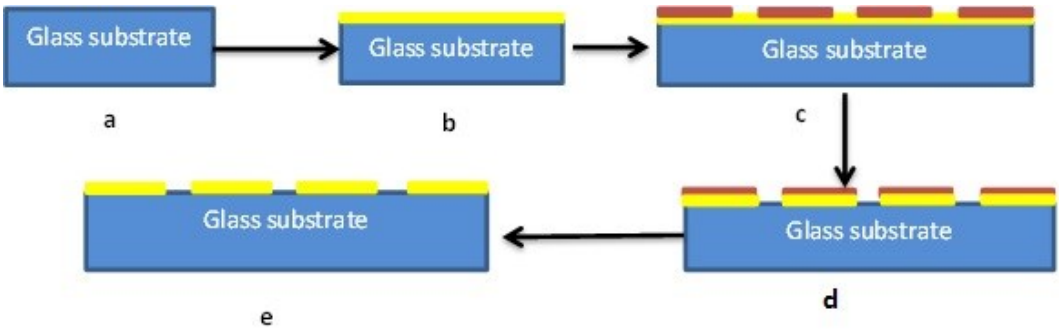

Figure 3.3 Fabrication process of IDE on glass substrate a)glass substrate b) Chrome/ Gold deposition 30/70nm as seed layer c) Electro plating of Gold up to 1.5 um and lithography d)Gold/ Chrome wet etching e) Acetone wash and drying

3.2.2.6. Gas measurements

The schematic diagram of the experimental setup is shown in figure 3.2. The measurement setup included: standard gases (2.5 vol% CH_4 and dry N_2), MFCs, sealed gas flow cell, sensor, tubings and an Impedance Analyzer (Agilent 429A) which was connected to a computer using a GPIB cable.

All the gas sensitivity characteristics of the Pd-SWCNTs were tested at room temperature. The flow cell had a normal atmospheric pressure and constant flow rate of 400 sccm during all the experiments.

The response of sensor S can be defined as [1], [4], [5]:

$$S = \frac{\Delta R}{R_{N_2}} = \frac{R_G - R_{N_2}}{R_{N_2}} \quad (3.1)$$

Where R_{N_2} is the resistance of the sensor measured in dry N_2 prior to methane exposure and R_G is the resistance after methane exposure. All the resistance values are recorder after the system has stabilized.

3.3. Results and discussion

3.3.1. Pd-SWCNT nanostructure characterization

Acid treatment of SWCNTs with concentrated HNO_3 plays an important role in the fabrication of Pd-SWCNT nanostructure. Halder et al. [13] have reported that surface functionalization of CNTs not only affects the attachment of metal nanoparticles on the surface of tubes, but also plays an important role on the catalytic activity which is related to the active sites of the CNT surface.

FE-SEM and TEM images of Pd-SWCNT nanostructures are displayed in figure 3.4 and 3.5 respectively. The SWCNTs shown in the images had larger diameter than that of single SWCNTs reported by the manufacturer. This may come from the fact that CNTS tend to aggregate as soon as they are removed from the ultrasonic bath as they poses highly hydrophobic surfaces [14].

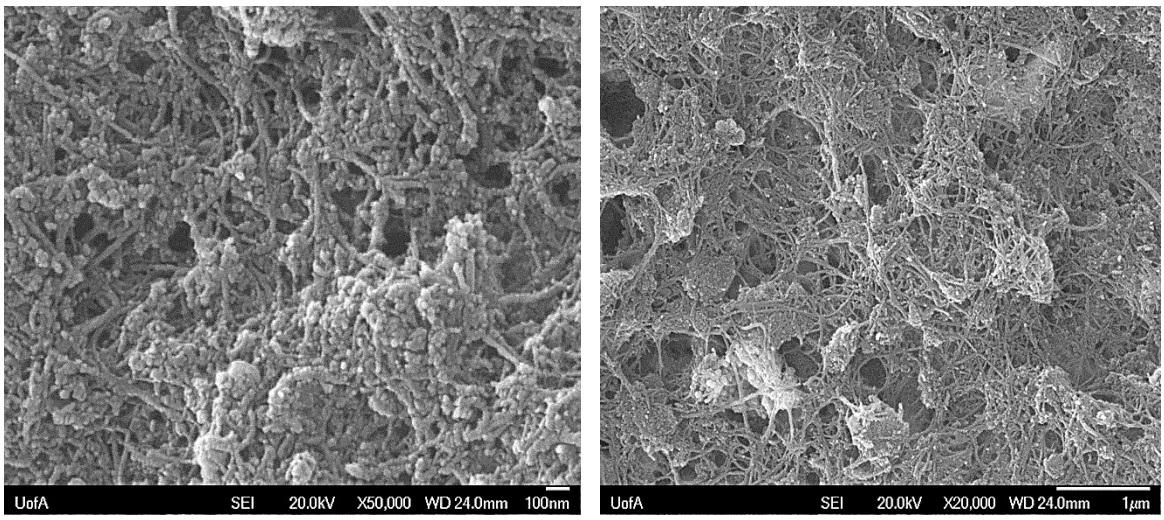

a **b**

Figure 3.4 SEM images of Pd-SWCNT nanostructures. The bright spots in figure (a) are Pd particles. The scale bar represents 100 nm for **a** and 1μm for **b**.

The Pd nanoparticles which are shown in figure 3.4 had a diameter of 8±1 nm. TEM results suggest that deposition of Pd nanoparticles on acid treated SWCNTs is nonuniform. This can be attributed to the fact that carbon nanotubes can be partially oxidized during reflux process, if not any. CNT's hydrophobic surface results in formation of agglomerations once they are removed from ultarsonication and transferred for reflux process. Once agglomerations are formed, acid cannot get into them thus leaving the aggregates unmodified [14] which translates into having a nonuniform metal decorated CNTs as the incorporation of Pd nanoparticles into the nonfunctionalized CNTs is found to be infinitesimal [12].

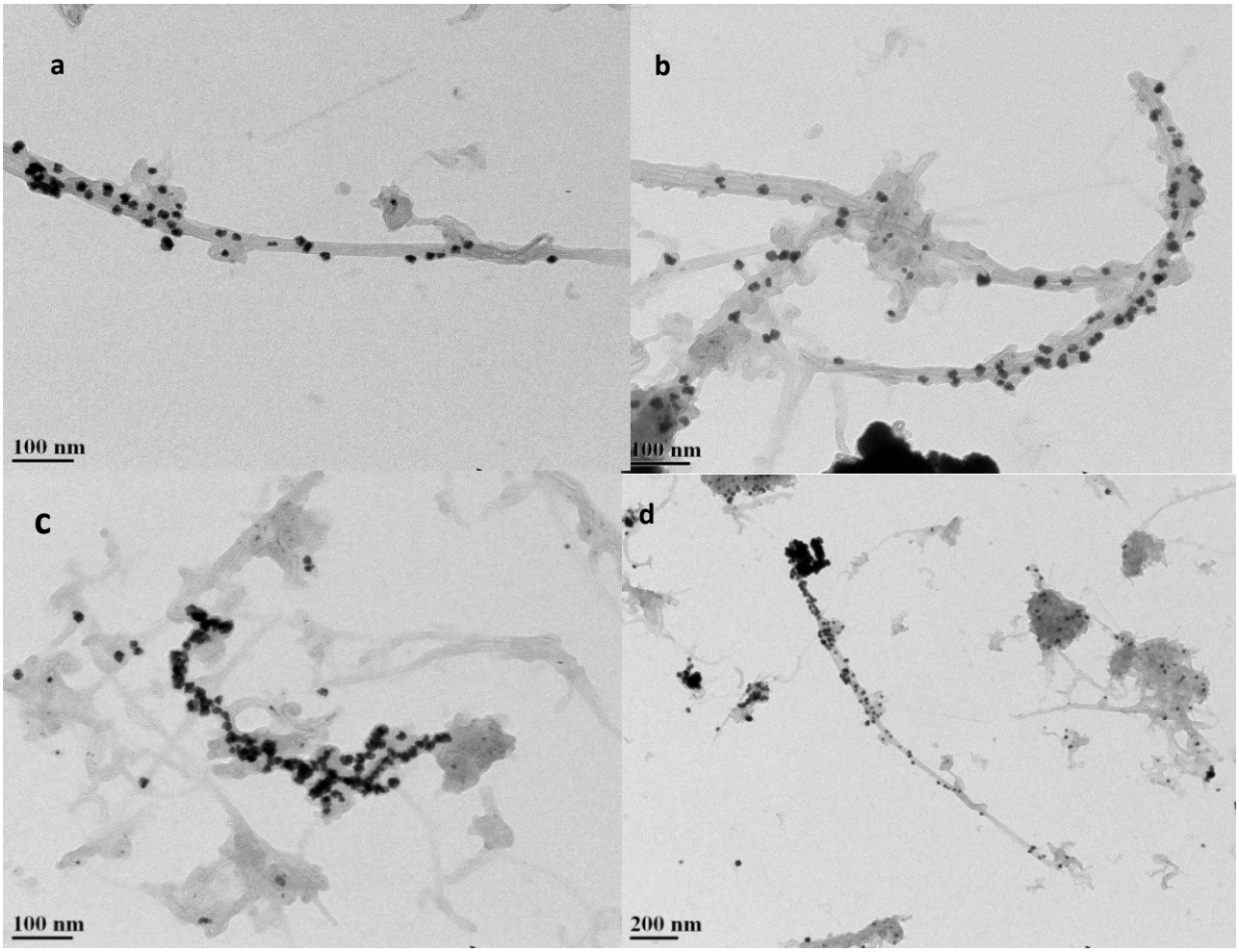

Figure 3.5 TEM images of Pd-SWCNT nanostructures. The black dots are Pd particles with measured average size of 8 nm. Scale bar represents 100 nm for **a, b, c** and 200 nm for **d**

3.3.2. Gas response of sensor

The response of the sensor was measured at room temperature. Figure 3.6 shows the response values of the sensor for different methane concentrations ranging from 1-2.5 vol% (10000-25000 ppm). As it is seen from the graph, the response of sensor increases as the concentration of methane increases. It was noticed that the response of sensor was reversible during each cycle.

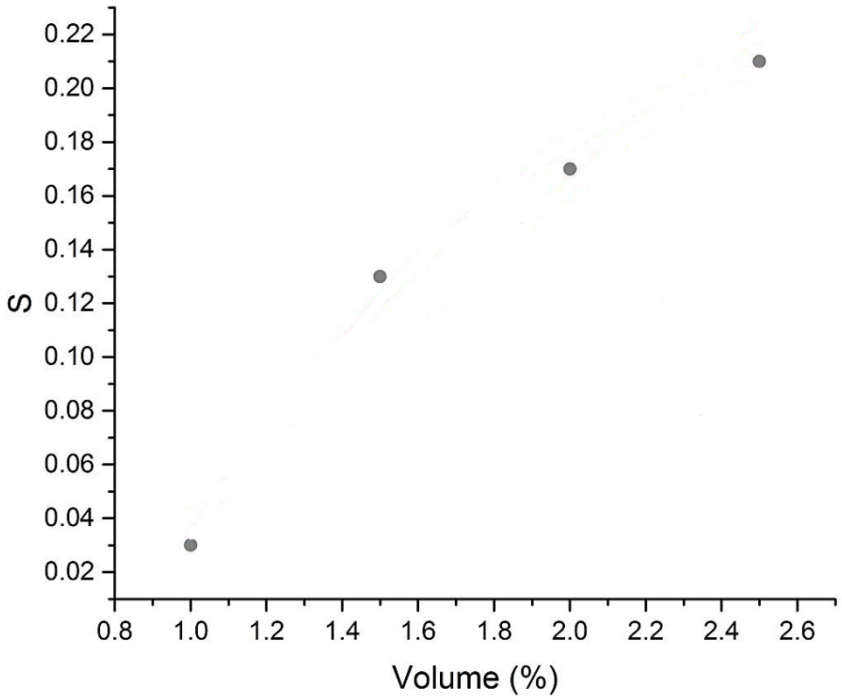

Figure 3.6 Response values (S) of Pd-SWCNT nanostructure exposed to different methane concentrations

The experiments suggested that the SWCNTs were insensitive to methane despite the fact that SWCNTs have large specific area which makes them suitable for adsorption of methane. However, inert properties of methane makes it unable to undergo any charge transfer reaction with SWCNTs at room temperature, thus there will be no change in electrical properties. Hence, SWCNTs alone cannot be used as methane sensors at room temperature [4].

The mechanism proposed by Lu et al. in [4] suggests that Pd attracts electrons from SWCNTS upon adsorption of methane in the Pd-SWCNT hence forming a weakly bound complex of $Pd^{\delta+}(CH_4)^{\delta-}$. SWCNTs consist of a single layer of a carbon. Therefore, all the atoms can be exposed to the environment and absorb gas molecules. In case of Pd-SWCNT and methane, H atoms in methane have a tendency to attract electrons from Pd. On the other hand, the Pd nanoparticles which are loaded on the SWCNT can get electrons from SWCNTs and aid in formation of the complex which leads to creation of more holes in the SWCNT[4]. This mechanism is demonstrated in figure 3.7.

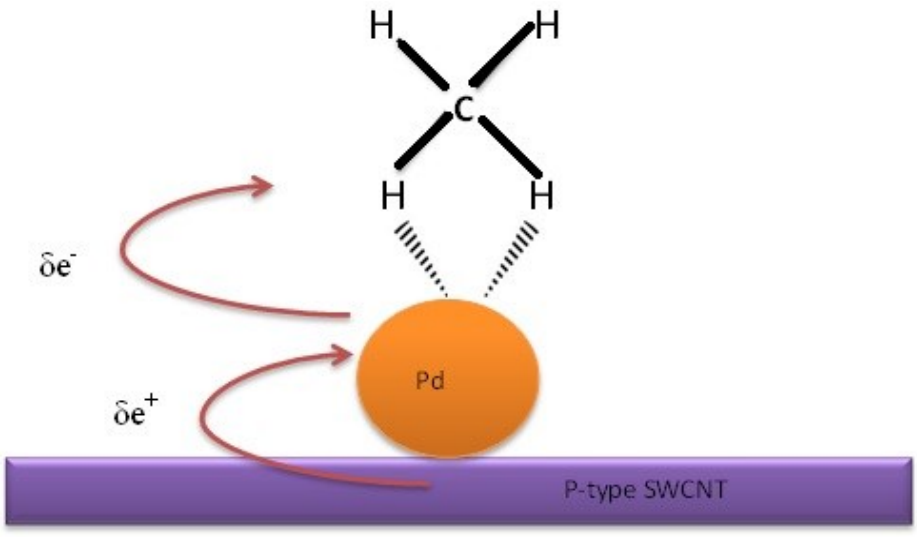

Figure 3.7 Sensing mechanism of room temperature methane detection with Pd-SWCNT

3.4. Summary

In summary, we have demonstrated a Pd-SWCNT sensor that has the potential of detecting methane at room temperature. The Pd nanoparticles were synthesized via chemical reduction of the precursor (Pd^{2+}) and had a diameter of 8±1 nm that was in good agreement with reported literature.

3.5. References

[1] Y. Li, H. Wang, Y. Chen, and M. Yang, "A multi-walled carbon nanotube/palladium nanocomposite prepared by a facile method for the detection of methane at room temperature," *Sensors Actuators B Chem.*, vol. 132, no. 1, pp. 155–158, May 2008.

[2] a Biaggi-Labiosa, F. Solá, M. Lebrón-Colón, L. J. Evans, J. C. Xu, G. Hunter, G. M. Berger, and J. M. González, "A novel methane sensor based on porous SnO2 nanorods: room temperature to high temperature detection.," *Nanotechnology*, vol. 23, no. 45, p. 455501, Nov. 2012.

[3] Z. P. Li, Y. Guo, S. Z. Wu, S. M. Shuang, and C. Dong, "Methane sensor based on palladium/MWNT nanocomposites," *Chinese Chem. Lett.*, vol. 20, no. 5, pp. 608–610, May 2009.

[4] Y. Lu, J. Li, J. Han, H.-T. Ng, C. Binder, C. Partridge, and M. Meyyappan, "Room temperature methane detection using palladium loaded single-walled carbon nanotube sensors," *Chem. Phys. Lett.*, vol. 391, no. 4–6, pp. 344–348, Jun. 2004.

[5] R. K. Roy, M. P. Chowdhury, and a. K. Pal, “Room temperature sensor based on carbon nanotubes and nanofibres for methane detection,” *Vacuum*, vol. 77, no. 3, pp. 223–229, Feb. 2005.

[6] F. Quaranta, R. Rella, P. Siciliano, S. Capone, M. Epifani, and L. Vasanelli, “A novel gas sensor based on SnO 2 r Os thin film for the detection of methane at low temperature,” pp. 350–355, 1999.

[7] E. Cordos, L. Ferenczi, S. Cadar, S. Costiug, G. Pitl, A. Aciu, and A. Ghita, “Methane and Carbon Monoxide Gas Detection system based on semiconductor sensor,” *2006 IEEE Int. Conf. Autom. Qual. Testing, Robot.*, vol. 2, pp. 208–211, May 2006.

[8] M. E. Cong, S. H. Guo, and Y. I. Wang, “A novel methane detection system based on InGaAsP distributed feedback laser,” vol. XLI, no. 3, 2011.

[9] O. Hennig, R. Strzoda, E. Mágori, E. Chemisky, C. Tump, M. Fleischer, H. Meixner, and I. Eisele, “Hand-held unit for simultaneous detection of methane and ethane based on NIR-absorption spectroscopy,” *Sensors Actuators B Chem.*, vol. 95, no. 1–3, pp. 151–156, Oct. 2003.

[10] Y. Jiang and C. Tang, “An optical fiber methane sensing system employing a two-step reference measuring method,” *Sensors Actuators B Chem.*, vol. 133, no. 1, pp. 174–179, Jul. 2008.

[11] Z. Wu, X. Chen, S. Zhu, Z. Zhou, Y. Yao, W. Quan, and B. Liu, “Room Temperature Methane Sensor Based on Graphene Nanosheets / Polyaniline Nanocomposite Thin Film,” vol. 13, no. 2, pp. 777–782, 2013.

[12] L. Meng, J. Jin, G. Yang, T. Lu, H. Zhang, and C. Cai, “Nonenzymatic electrochemical detection of glucose based on palladium-single-walled carbon nanotube hybrid nanostructures.,” *Anal. Chem.*, vol. 81, no. 17, pp. 7271–80, Sep. 2009.

[13] A. Halder, S. Sharma, M. S. Hegde, and N. Ravishankar, “Controlled Attachment of Ultrafine Platinum Nanoparticles on

Functionalized Carbon Nanotubes with High Electrocatalytic Activity for Methanol Oxidation," *J. Phys. Chem. C*, vol. 113, no. 4, pp. 1466–1473, Jan. 2009.

[14] Y. Xing, "Synthesis and Electrochemical Characterization of Uniformly-Dispersed High Loading Pt Nanoparticles on Sonochemically-Treated Carbon Nanotubes," *J. Phys. Chem. B*, vol. 108, no. 50, pp. 19255–19259, Dec. 2004.

Chapter 4: Conclusions and Future work

4.1. Conclusions

Detection of methane at room temperature is of great importance because of several factors such as being combustible at certain concentrations (LEL: 5-15 vol %) and ranking the second greenhouse gas. Hence, the need for having a reliable gas sensor that can detect methane at room temperature is increasing. Two different approaches that have been discussed through this thesis provide promising platforms to fulfill the need for such methane sensor.

The first approach in which a microcantilever along with a quantum cascade laser have been utilized, provides an accurate yet fast method for detection of methane at room temperature without using any chemoselective interface. Thus, the sensor needs less regeneration as there is no coating on the surface to be degraded. Here, we were able to get the fingerprint of methane for different concentrations (from 2.5 Vol% down to 0.083 vol%) that are well below the LEL of methane. According to the theoretical models, the absorbed amount of methane on the cantilever is less than pico gram. However, the PCDS system could detect it.

The second method used for developing the sensor, Pd-SWCNT coated interdigitated electrode, also offers a reliable yet cost effective method to detect methane at room temperature. In this study Pd nanoparticles were synthesized via a chemical reduction of the precursor. The synthesis method offered a simple way for synthesis of particles with average diameter of 8±1 nm that were in excellent agreement with the reported literature. TEM images showed that incorporation of Pd nanoparticles into the SWCNTs were successful. The sensor showed increasing response as the concentration of methane increased through the flow cell.

4.2. Future works

As shown in this study, there is a promise for making a handheld device using PCDS technique for the real time detection of methane. The amount of mass adsorbed on the cantilever also could be quantified by the experiments using nano cantilevers that have higher frequency. However, further studies are needed to confirm the potential of this technique to be used as a real time sensing device.

The preliminary results with SWCNTs incorporated with palladium nanoparticles also suggest the potential of using CNTs as a platform

for room temperature methane sensing. Yet, more studies are needed to improve the detection limit and also overall response of sensor.